

Spectral Energy Distribution analysis of Fermi-LAT bright blazars from radio to GeV energies

M.N. Mazziotta[§], P. Giommi^{*}, S. Cutini^{*}, D. Gasparrini^{*}
 and C. Monte^{‡,§} on behalf of the Fermi-LAT collaboration,
 L. Fuhrmann and E. Angelakis[¶] on behalf of the F-GAMMA team,
 M. Villata^{||} and C.M. Raiteri^{||} on behalf of the GASP-WEBT collaboration,
 M. Perri^{**} on behalf of the Swift-XRT collaboration,
 J. Richards^{††} on behalf of the OVRO 40m team

[§]*Istituto Nazionale di Fisica Nucleare, Sezione di Bari, I-70126, Bari, Italy*

^{*}*Agenzia Spaziale Italiana (ASI) Science Data center I-00044 Frascati (Roma), Italy*

[‡]*Dipartimento di Fisica "M. Merlin" dell'Università e del Politecnico di Bari, I-70126 Bari, Italy*

[¶]*Max-Planck-Institut fuer Radioastronomie Auf dem Huegel 69, Bonn 53121, DE*

^{||}*INAF, Osservatorio Astronomico di Torino I-10025, Torino, Italy*

^{**}*Agenzia Spaziale Italiana (ASI) Science Data center I-00044 Frascati (Roma), Italy*

^{††}*California Institute of Technology, Pasadena, California, USA*

Abstract. The Large Area Telescope (LAT), the main instrument on-board the Fermi Gamma-ray Space Telescope (formerly GLAST, launched June 11, 2008) is a pair conversion detector designed to study the gamma-ray sky in the energy range from 20 MeV to >300 GeV. We present the preliminary results of a Spectral Energy Distribution Analysis performed on a sample of bright blazars detected in the first three months of data collection of Fermi. The analysis is extended down to radio, optical, UV and X-ray bands and up to GeV energies based on unprecedented sample of simultaneous multi-wavelength observations.

Keywords: Spectral Analysis, Gamma-Rays, Galaxies

I. INTRODUCTION

The Gamma-ray Large Area Space Telescope (GLAST) satellite was successfully launched on June, 11 2008 into a low Earth circular orbit at an altitude of 550 km and an inclination of 25.6° . At the end of its commissioning phase (August, 4 2008), after entering its scientific operating mission, the satellite was renamed Fermi. The Large Area Telescope (LAT) on board Fermi is a pair-production telescope with large effective area (~ 8000 cm² on axis for $E > 1$ GeV) and field of view (~ 2.4 sr at 1 GeV), sensitive to gamma-rays in the energy range 20 MeV to >300 GeV [1].

One of the major scientific goal of the Fermi mission is to provide new data about gamma-ray emission from Active Galactic Nuclei (AGNs). During the first three months of sky-survey operation, the Fermi Large Area Telescope (Fermi-LAT) detected 132 bright sources at $|b| > 10^\circ$ with test statistic greater than 100 (corresponding to about 10σ). Among these, 106 high-confidence associations with known AGNs have been found. This sample is referred as the LAT Bright AGN Sample (LBAS) [2].

For 48 sources of the LBAS, we were able to combine LAT three months gamma-ray data with simultaneous observations at other wavelengths [3]. In particular, radio data come from OVRO (Owens Valley Radio Observatory) 40 -m telescope (15 GHz) [4], Effelsberg 100 -m Radio Telescope (2.6 to 42 GHz, F-GAMMA project [5]), and GASP-WEBT (5 to 43 GHz and 23 to 345 GHz) [6]. NIR-optical data come from GASP-WEBT collaboration; optical/UV data come from the Swift 30 cm modified Ritchey-Chretien Ultraviolet/Optical Telescope (UVOT) [7] and X-ray data come from the Swift X-Ray Telescope (XRT) [8].

II. PHYSICAL CLASSIFICATION OF AGNS

The radiation emitted by AGNs is attributed to one (or both) of the following physical processes:

- thermal emission originating from infalling material strongly heated in the inner parts of the accretion disk close to the black hole;
- non-thermal emission emitted in a magnetic field by highly energetic particles that have been accelerated in a jet of material ejected from the nucleus at relativistic speed.

The first process produces radiation mostly in the optical, UV and X-ray band, whereas radiation produced through the second mechanism is emitted across the entire electromagnetic spectrum. In particular, AGNs where non-thermal processes are energetically dominant at all frequencies are named Non-Thermal radiation dominated AGNs (NT-AGN).

The NT-AGNs can be subdivided into Blazars, that are core-dominated flat or inverted radio spectrum NT-AGN, and Misdirect NT-AGNs, that usually show very extended, double-sided radio jets/lobes pointing in opposite directions in the plane of the sky with respect to the central nucleus.

Blazars are further divided into:

- BZQ (or *Blazars of the QSO type*), i.e. blazars that show broad emission lines in their optical spectrum just like normal QSO (Quasi Stellar Objects). This category includes objects normally referred as Flat Spectrum Radio Quasars (FSRQs) and broad-line radio galaxies.
- BZB (or *Blazars of the BL Lac type*), i.e. blazars similar to the BL Lacertae objects, with no strong lines in their optical spectrum.
- BZU (or *Blazars of the Unknown type*), i.e. blazars which do not have optical spectra sufficiently defined to determine precisely the presence of broad emission lines or their width.

BL Lac objects, fall into two categories [9], defined as *Low-frequency peaked BL Lacs* (LBL) and *High-frequency peaked BL Lacs* (HBL) depending on the ratio:

$$\alpha_{rx} = \log(F_{5\text{ GHz}}/F_{1\text{ keV}})/7.68$$

is greater than or less than 0.75, respectively. In the previous equation, $F_{5\text{ GHz}}$ and $F_{1\text{ keV}}$ are respectively the measured radio flux at 5 GHz and the measured X-ray flux at 1 keV.

The observed differences in continuum multiwavelength spectral shape are:

- the synchrotron power of LBL peaks at radio to IR wavelengths while that of HBL peaks at UV to X-ray wavelengths;
- the Compton components peak at GeV energies for LBL and at much higher (TeV) energies for HBL.

The continuum spectra of FSRQ are very similar to those of LBL with synchrotron peak at $10^{13} \div 10^{14}$ Hz and Compton peak at $10^{22} \div 10^{23}$ Hz [9].

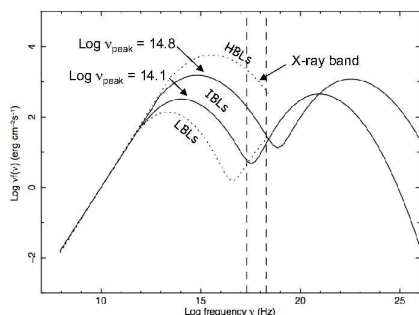


Fig. 1: Scheme of NT-AGN classification.

The usual BL Lac objects classification described above can be extended to all NT-AGNs (see Fig. 1) as follows:

- LBL (or *Low energy peaked NT-AGNs*): for these sources, the synchrotron peak is located at low energies, i.e. in the far IR or IR band ($\nu_{peak} < 10^{14.1}$ Hz) and therefore their X-ray emission is flat, due to the rising part of the inverse Compton component.

- HBL (or *High energy peaked NT-AGNs*): the emitting particles are accelerated at much higher energies than in LBLs and consequently the synchrotron peak power reaches UV or higher energies ($\nu_{peak} > 10^{14.8}$ Hz) and under these conditions, the synchrotron emission dominates the observed flux in the X-ray band;
- IBL (or *Intermediate energy peaked NT-AGNs*): for these sources, the synchrotron emission peaks at intermediate energies ($10^{14.1} < \nu_{peak} < 10^{14.8}$ Hz). In this case the X-ray band includes both the tail of the synchrotron emission and the rise of the inverse Compton component.

III. LAT DATA SELECTION AND ANALYSIS

Fermi-LAT data from 4 August to 30 October 2008 have been analyzed, selecting for each source only photons belonging to the diffuse class (Pass6 V1 IRF) [1]. Events within a 15° Region of Interest (RoI) centered around the source to be analyzed have been selected. From each data sample photons with a zenith angle larger than 105° with respect to the Earth reference frame and events entering the LAT with an angle larger than 66.4° with respect to the Z-axis in the instruments reference frame have been excluded [10].

Two methods have been used to reconstruct the source energy spectra. In the first method the source spectrum as well as the diffuse background components are assumed to be described by a model, that depends on a set of free parameters. Then a maximum likelihood approach (*gtlike*) [11] has been implemented to estimate the parameters in each individual energy bin, and the flux of the source under investigation is evaluated. It is worth to point out that this method does not take into account energy dispersion and correlations among the energy bins.

In the second method a deconvolution (unfolding) technique [12] has been used to reconstruct the source energy spectra from the observed data, after background subtraction. This method allows to reconstruct the source spectra from the observed data without assuming any spectral model, taking also into account the finite energy dispersion of the detector. The purpose of the unfolding is to estimate the true distribution (in this case the true source energy spectrum), given the observed one and assuming the knowledge of the smearing matrix, which describes the migration effects among the energy bins as well as the efficiencies. The results of the two different methods are consistent.

Once the differential flux in each energy bin $\phi(E)$ has been evaluated, the corresponding Spectral Energy Distribution (SED) is then obtained multiplying the differential flux in each energy bin for the square of the central energy value of that bin, i.e. $\nu F(\nu) = E^2 \phi(E)$ where $E = h\nu$.

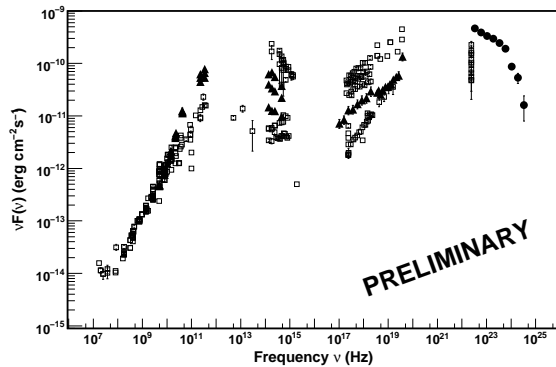


Fig. 2: SED of 3C 454.3 FSRQ. Open squares: historical SED data; Filled circles: LAT SED data; Filled triangles: simultaneous SED data at other wavelengths.

IV. SIMULTANEOUS OBSERVATIONS AT OTHER WAVELENGTHS

The Swift Ultraviolet/Optical Telescope (UVOT) is sensitive in the $170 \div 650$ nm band. The UVOT produces a series of images in a series of lenticular filters. The photometric analysis of the 48 sources was performed using the standard UVOT software distributed within HEASoft6.3.2 package and the calibration included in the latest release of the “Calibration Database”. Counts were extracted from aperture of $5''$ radius for all filters and then converted to fluxes.

The Swift X-Ray Telescope (XRT) is sensitive in the energy range $0.2 \div 10$ keV. The XRT data were reduced using the XRTDAS software (v6.5) developed at the ASI Science Data Center (ASDC) and distributed within the HEASoft 6.6.1 package by NASA High Energy Astrophysics Archive Research Center (HEASARC). Only photons with grades in the range $0 \div 12$ were selected and the default screening parameters were used in order to produce level 2 cleaned event files. X-ray images were accumulated from events previously cleaned and calibrated. Only photons with energy between 0.3 and 10 keV were accepted. Source count rates were estimated using the DETECT routine within the XIMAGE.V 4.2 package. Net counts were then converted into flux assuming a power law spectrum with photon index equal to 1.5 and setting the amount of photoelectric absorption equal to the Galactic value along the line of sight.

The quasi-simultaneous Effselberg radio observations were conducted with cross-scans in azimuth/elevation with the number of sub-scans matching the source brightness at the given frequencies. The individual spectra were measured quasi-simultaneously within ≤ 40 minutes rapidly switching between the different secondary focus receivers. The data reduction was done applying standard procedures and post-observational corrections including opacity correction, pointing offset correction, gain correction and sensitivity correction [13].

The GLAST-AGILE Support Program (GASP) was born from the Whole Earth Blazar Telescope (WEBT) [6] and started its operation in September 2007, with the aim of performing long-term optical-to-radio monitoring of 28 gamma-loud blazars, to compare the low-energy flux behaviour with the behaviour observed at gamma-ray energies. In the period considered in this analysis, the GASP carried out ~ 3000 optical observations as well as near-IR and radio observations of 19 LBAS blazars. In the SED shown here we report the average, minimum and maximum values at each observed frequency

Quasi-simultaneous 15 GHz observations with the Owens Valley Radio Observatory (OVRO) 40 - m radio telescope were made as part of an ongoing Fermi-LAT blazar monitoring program, wherein ~ 1200 blazars are observed twice per week. The OVRO flux densities are measured in a single 3 GHz wide band centered on 15 GHz. Observations were performed using azimuth double switching as described in Ref. [14], which removes much atmospheric and ground interference. The relative uncertainties in flux density result from a 5 mJy typical thermal uncertainty in quadrature with a 1.6% systematic uncertainty. The absolute flux density scale is calibrated to about 5% via observations of the steady calibrator 3C 286.

V. BLAZAR SPECTRAL ENERGY DISTRIBUTIONS

Since AGN are highly variable objects, simultaneous observations in different energy bands are essential in order to understand the emission processes that take place in these objects. The complete SED, based on simultaneous data is also very important in order to classify the NT-AGNs in HBL, IBL or LBL.

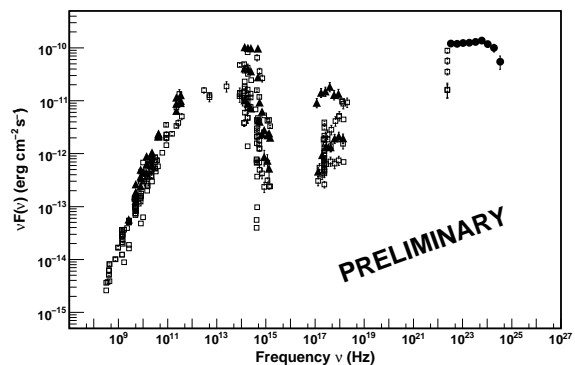


Fig. 3: SED of AO 0235+164 LBL. Open squares: historical SED data; Filled circles: LAT SED data; Filled triangles: simultaneous SED data at other wavelengths.

As said before, for 48 sources of the LBAS, we were able to combine Fermi-LAT three months gamma-rays data with simultaneous observations at other wavelengths. In the following, three examples of SED for blazars belonging to different classes will be shown [3]. In these plots open square points represent historical SED data (not simultaneous with respect to Fermi-LAT

data) at different wavelengths, while filled points represent simultaneous SED data from Fermi-LAT (circles) and at other wavelengths (triangles).

Fig. 2 shows the SED of the well-known Flat Spectrum Radio Quasar 3C 454.3 ($RA = 343.5^\circ$, $DEC = 16.151^\circ$, $z = 0.859$). The 3C 454.3 can be considered as an example of FSRQ-LBL.

Fig. 3 shows the SED of the AO 0235+164 source ($RA = 39.663^\circ$, $DEC = 16.613^\circ$, $z = 0.94$). This source can be considered as an example of BLLac-LBL.

Fig. 4 shows the SED of the W Comae source ($RA = 185.438^\circ$, $DEC = 28.243^\circ$, $z = 0.102$), that is an example of IBL.

Some of the gamma-ray spectra show breaks or curvatures as pointed out in Ref. [2]. In particular, the observed gamma-ray spectrum for the 3C 454.3 is not consistent with a simple power-law, but instead steepens strongly above about 2 GeV [16].

VI. DISCUSSION AND CONCLUSIONS

By combining the Fermi data with radio (OVRO, Effelsberg and GASP-WEBT), NIR-optical (GASP-WEBT), Optical-UV (Swift UVOT) and X-ray (Swift XRT) data we were able to assemble quasi-simultaneous SED for 48 LBAS blazars. The SED of these sources are similar to those of blazars discovered at other wavelengths (e.g. radio or X-ray), clearly showing the typical two-bump signature usually attributed to Synchrotron and inverse Compton emission. We have used these SEDs to estimate the position of the peak of the Synchrotron and inverse Compton power and intensities. Our data show that the synchrotron peak is located between $10^{12.5}$ Hz and 10^{14} Hz in BZQ and it can reach 10^{16} Hz and 10^{17} Hz for BZB.

The γ -ray spectral slope is strongly correlated with the synchrotron peak energy (ν_{peak}^{sync}), as expected in Synchrotron Self Compton (SSC) models; however simple homogeneous SSC models cannot explain most of our SEDs, especially in the case of LBL sources. Since the

LAT detector is more sensitive to flat spectrum γ -ray sources, the correlation between ν_{peak}^{sync} and spectral index strongly favors the detection of hard γ -ray sources thus explaining the Fermi-LAT overabundance of high energy peaked blazars compared to radio and EGRET samples. This selection effect will be even stronger above a few GeV reproducing the case of the soft X-ray band where HBL BL Lacs are the dominant type of blazars. The full analysis and results will be reported in the forthcoming paper [3].

ACKNOWLEDGMENTS

The *Fermi* LAT Collaboration acknowledges support from a number of agencies and institutes for both development and the operation of the LAT as well as scientific data analysis. These include NASA and DOE in the United States, CEA/Irfu and IN2P3/CNRS in France, ASI and INFN in Italy, MEXT, KEK, and JAXA in Japan, and the K. A. Wallenberg Foundation, the Swedish Research Council and the National Space Board in Sweden. Additional support from INAF in Italy for science analysis during the operations phase is also gratefully acknowledged. This research is based also on observations with the 100 m telescope of the MPIfR (Max-Planck-Institut für Radioastronomie) at Effelsberg. The OVRO 40 m program is supported in part by NASA (NNX08AW31G) and the NSF (AST-0808050).

REFERENCES

- [1] W.B. Atwood et al., *The Large Area Telescope on the Fermi Gamma-ray Space Telescope Mission*, ApJ 697 (2009) 1071, arXiv:0902.1089v1[astro-ph.IM]
- [2] A.A. Abdo et al., *Bright AGN Source List from Three Months of the Fermi Large Area Telescope Sky Survey*, arXiv:0902.1559v1[astro-ph.HE]
- [3] A.A. Abdo et al., *The Spectral Energy Distributions of Fermi bright blazars*, To be submitted to Astrophysical Journal
- [4] <http://www.oato.inaf.it/blazars/web/>
- [5] L. Fuhrmann et al., *The First GLAST Symposium*, 921, 249 (2007)
- [6] <http://www.oato.inaf.it/blazars/web/>
- [7] P.W.A. Roming et al., *The Swift Ultra-Violet/Optical Telescope*, Space Science Reviews, 120 (2005), 95
- [8] D.N. Burrows et al., *The Swift X-Ray Telescope*, Space Science Reviews, 120 (2005), 165
- [9] C. M. Urry, *Multiwavelength properties of blazars*, Advances in Space Research, 21 (1998), 89
- [10] A.A. Abdo et al., *Fermi Large Area Telescope Bright Gamma-ray Source List*, arXiv:0902.1340v1[astro-ph.HE]
- [11] <http://fermi.gsfc.nasa.gov/ssc/data/analysis/documentation/Cicerone>
- [12] M.N. Mazziotta, *A method to unfold the energy spectra of point like sources from the Fermi-LAT data*, these proceedings
- [13] E. Angelakis et al. *Memorie della Societa Astronomica Italiana*, 79, 1042 (2008)
- [14] Readhead et al., ApJ, 346, 566 (1989)
- [15] V. A. Acciari and the VERITAS Collaboration, *The Astrophysical Journal* **684** (2008) L73
- [16] A.A. Abdo et al., *Early Fermi Gamma-ray Space Telescope observations of the blazar 3C 454.3* Astrophysical Journal 2009 in press, arXiv: 0904.4280 <http://www.arxiv.org/abs/0904.4280>

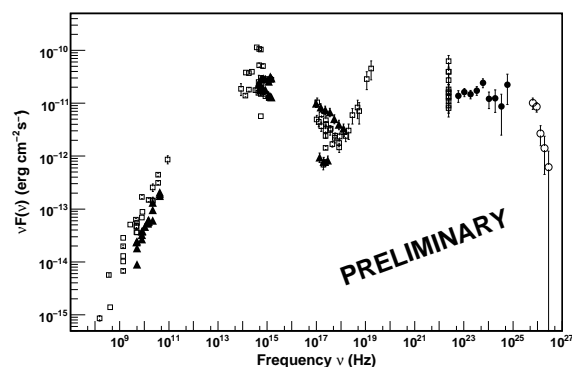


Fig. 4: SED of W Comae IBL. Open squares: historical SED data; Filled circles: LAT SED data; Filled triangles: simultaneous SED data at other wavelengths. Open circles: VERITAS results [15].